Characterization of Natural Organic Matter in Bentonite Clays

NWMO TR-2014-10 May 2014

Michaela H.M. Marshall and Myrna J. Simpson

University of Toronto

Nuclear Waste Management Organization
22 St. Clair Avenue East, 6th Floor
Toronto, Ontario
M4T 2S3
Canada

Tel: 416-934-9814
Web: www.nwmo.ca

Characterization of Natural Organic Matter in Bentonite Clays

NWMO TR-2014-10

May 2014

Michaela H.M. Marshall and Myrna J. Simpson
University of Toronto

Document History

Title:	Characterization of Natural Organic Matter in Bentonite Clays		
Report Number:	NWMO TR-2014-10		
Revision:	R000	Date:	May 2014
University of Toronto			
Authored by:	Michaela H.M. Marshall		
Verified by:	Myrna J. Simpson		
Approved by:	Myrna J. Simpson		
Nuclear Waste Management Organization			
Reviewed by:	Jennifer McKelvie Peter Keech Ken Birch Alan Murchison		
Accepted by:	Chris Hatton		

ABSTRACT

Title: **Characterization of Natural Organic Matter in Bentonite Clays**
Report No.: **NWMO TR-2014-10**
Authors: Michaela H.M. Marshall and Myrna J. Simpson
Company: University of Toronto
Date: May 2014

Abstract

The Canadian concept for a deep geological repository (DGR) involves multiple barriers to contain and isolate used nuclear fuel. The DGR concept relies on both natural and engineered barriers. Highly compacted bentonite clay surrounding the used fuel container is one of the engineered barriers in this proposed system. While many of the mechanical and physical properties of bentonite clays have been characterized, the composition of the natural organic matter (NOM) present in these clays is not well understood.

The geochemistry of clay samples from Wyoming, Saskatchewan, Greece and India were characterized. Molecular-level methods including biomarker analysis, solid-state ^{13}C Nuclear Magnetic Resonance (NMR) and solution-state ^{1}H NMR were then used to more closely study the structure and source of NOM in clays from Wyoming and Saskatchewan.

The aliphatic lipid distribution was mainly composed of biomarkers from microbes and vascular plants with a higher concentration observed for vascular plant inputs. Lignin-derived NOM in one of the Wyoming samples was found to be in an advanced stage of oxidation based on the vanillyl acid to aldehyde ratio. The majority of the signal intensity in the solid-state ^{13}C NMR spectra was detected in the aromatic and aliphatic regions. The ratio of signal in the alkyl/*O*-alkyl regions ranged from 7.6 to 9.7 which corresponds to NOM that has undergone advanced diagenesis. The signal in the aliphatic region of the solid-state ^{13}C NMR spectra is thought to correspond to mainly long-chain compounds that do not have much side chain branching, such as long-chain plant waxes. This hypothesis was also confirmed with solution-state ^{1}H NMR analysis based on the higher intensity of the peak corresponding to CH_2 protons relative to the peak for CH_3 protons. The aromatic signal in the ^{13}C NMR spectra does not seem to correspond to lignin or proteins and may therefore be indicative of condensed aromatic carbon. The composition of NOM in the clays at the molecular-level did not vary much between clays.

NOM present showed signs of advanced degradation and the remaining NOM seems to be composed of compounds with a strong affinity for the clay surface (namely plant-derived waxes). This type of NOM is hypothesized to be more recalcitrant as compared to other labile NOM sources (sugars, proteins, and small organic acids) which were not detected.

TABLE OF CONTENTS

Page

ABSTRACT ..... **iii**

1. INTRODUCTION **1**

2. GEOCHEMICAL ANALYSIS **3**

2.1 MATERIALS **3**
2.2 METHODS **3**
2.2.1 Carbon Analysis 3
2.2.2 Nitrate and Nitrite 3
2.2.3 Inductive Coupled Plasma Optical Emission Spectrometry (ICP-OES) Analysis 4
2.2.4 Cation Exchange Capacity (CEC) 4
2.2.5 Heavy Metal Analysis 4
2.2.6 Sulfur 4
2.2.7 pH 4
2.2.8 Total Nitrogen 4
2.2.9 Extractable Phosphorous 5
2.3 GEOCHEMICAL ANALYSIS RESULTS **5**
2.4 DISCUSSION OF GEOCHEMICAL ANALYSIS **7**

3. MOLECULAR-LEVEL ANALYSIS OF NATURAL ORGANIC MATTER IN CLAY SAMPLES **7**

3.1 MATERIALS **7**
3.2 METHODS **8**
3.2.1 Chemical Extractions and GC-MS Analysis 8
3.2.2 Detection and Quantification Limits 9
3.2.3 Solid-State ^{13}C NMR 9
3.2.4 Solution-State NMR 9
3.3 RESULTS OF NOM MOLECULAR LEVEL ANALYSIS **10**
3.3.1 Chemical Extractions and GC-MS Analysis 10
3.3.2 Solid-State ^{13}C NMR 16
3.3.3 Solution-State ^{1}H NMR 17
3.4 DISCUSSION OF MOLECULAR ANALYSIS **20**

4. CONCLUSIONS **23**

ACKNOWLEDGEMENTS **23**

REFERENCES **24**

LIST OF TABLES

Page

Table 1: Geochemical Characterization of Clay Samples 6
Table 2: Comparison of Geochemical Literature Values 7
Table 3: GC-MS Detection Limits for Representative Biomarker Compounds 10
Table 4: Major Components of NOM (ng/g Clay) and Their Sources Identified After Solvent Extraction of MX-80, National and CCP Clays 11
Table 5: Major Components of NOM (ng/g Clay) and Their Sources Identified After Base Hydrolysis of MX-80, National and CCP Clays 14
Table 6: Major Components of NOM (ng/g Clay) and Their Sources After CuO Oxidation of MX-80, National and CCP Clays 15
Table 7: Relative Abundance (%) of Solid-State ^{13}C NMR Signal for Different Structural components of NOM 17
Table 8: Carbon and Proton Pairs Identified in Clay Sample CCP and Corresponding Chemical Shifts (Deshmukh et al., 2003; Simpson et al., 2003). 17

LIST OF FIGURES

Page

Figure 1: The Engineered Barrier System Conceptual Design (adapted from Villagran et al. 2011) 1
Figure 2: Solid-State CPMAS ^{13}C NMR Spectra of HF-Treated Clay Samples from Wyoming, USA and Saskatchewan, Canada showing the four major spectral regions: aliphatic, 0-50 ppm; *O*-alkyl, 20-110 ppm; aromatic & phenolic, 110-165 ppm and carboxyl & carbonyl, 165-220 ppm (Baldock et al., 1992; Simpson et al., 2008). 16
Figure 3: Solution-State ^{1}H NMR of the Base-Soluble Material Extracted from Clay Sample CCP. Highlighted Regions Correspond to the Following Protons: Aliphatic, 0.3-2.9 ppm; *O*-alkyl, 2.9-4.1 ppm; $\alpha^{1}H$ from proteins, 4.1-4.8 ppm; aromatic, 6.2-7.8 and amide, 7.8-8.4 (Clemente et al., 2012). Additional Peak Assignments (A_1, A_3, B_1, B_2, C_2, D_2 and E) are explained in Table 8. 18
Figure 4: Solution-State ^{1}H NMR of the Water-Soluble Material Extracted from Clay Sample CCP. Highlighted Regions Correspond to the Following Protons: Aliphatic, 0.3-2.9 ppm; *O*-alkyl, 2.9-4.1 ppm; $\alpha^{1}H$ from proteins, 4.1-4.8 ppm; aromatic, 6.2-7.8 and amide, 7.8-8.4 (Clemente et al., 2012). Additonal peak assignments (A_1, A_3, B_1 and B_2) are explained in Table 8. 19
Figure 5: ^{1}H-^{13}C HSQC NMR Spectrum of the Base-Soluble Material from Clay Sample CCP Highlighting Major ^{1}H-^{13}C Couplings Between Aliphatic and *O*-Alkyl Structures. Assignments are explained in Table 8. 20

1. INTRODUCTION

The Canadian concept for containment and isolation of used nuclear fuel consists of a multi-barrier system that includes both natural and engineered barriers (Villagran et al., 2011). The naturally-occurring barriers are geological in nature while the engineered barriers can be divided into the used nuclear fuel container and surrounding clay buffer, seal and backfill materials as shown in Figure 1. Overall, this deep geological repository (DGR) concept entails a network of tunnels and placement rooms located approximately 500 m below ground level in either an appropriate crystalline or sedimentary rock formation. During construction and operation, a shaft connecting the DGR to the surface will be used to transport the packaged used nuclear fuel to the repository level; this access will be sealed upon repository closure.

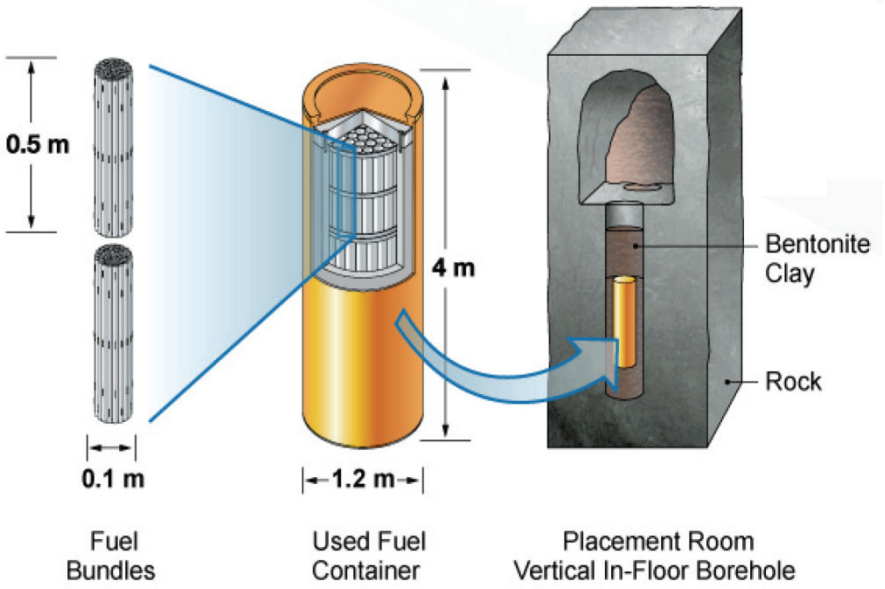

Figure 1: The Engineered Barrier System Conceptual Design (adapted from Villagran et al. 2011)

Bentonite clay has been chosen as the buffer material in DGR concepts (Kiviranta and Kumpulaninen, 2010; Mariner et al., 2011; Svensson et al., 2011; Wilson et al., 2011). The main function of the buffer is to protect the used fuel container (UFC) which encloses the used nuclear fuel bundles (Karnland, 2010) and prevents infiltration of groundwater (SKB, 2006; Wilson et al., 2011). The buffer is also responsible for minimizing microbial activity near the UFC and promoting retardation of radionuclides (Kiviranata and Kumpulainen, 2011). Bentonite clay is primarily composed of montmorillonite, a smectite mineral characterized by negatively charged surfaces and large spacing between clay layers (Keto, 2003). Many of the physical properties of bentonite have been studied by the NWMO and other organizations. The thermal, hydraulic and mechanical properties, as well as the swelling ability and cation exchange capacity have all been well characterized (Keto, 2003; Villagran et al., 2011; Wilson et al., 2011).. In the unlikely event of a failed container, the high sorption capacity of the negatively charged clay surface for cations including radionuclides will limit the release of these potentially harmful species into the environment (Bors et al., 1999; Kozai, 1998). Bentonite will also swell upon contact with water due to the large spacing between clay units. These clay interlayers can each accommodate several layers of water molecules (Hicks et al., 2009). Upon saturation with

groundwater, swelling of the buffer material will fill in any gaps that may be present between the buffer and UFC, improving the isolation of the spent nuclear fuel from the surrounding environment (Mariner et al., 2011).

High density bentonite clay also has sufficiently small pore sizes to discourage unwanted microbial activity in the vicinity of the UFC (Stroes-Gascoyne et al., 2010). However, at interfaces or other locations where the required density of the clay is not maintained, microbial activity may occur (Stroes-Gascoyne et al., 2011). Microbes can survive in various environments provided that their water, nutrient and energy requirements are met and that they can tolerate the environmental conditions (Stroes-Gascoyne and West, 1997). Natural organic matter (NOM) in the repository materials, such as that contained in bentonite clay, may serve as a nutrient source for microbes (Oscarson et al., 1986). NOM is found throughout the lithosphere, hydrosphere and atmosphere. It is composed of biologically derived organic compounds that have typically been chemically altered through biological processes (Baldock and Skjemstad, 2000). Microbial activity in the DGR may result in microbiological-mediated corrosion of the UFC because the activity of sulfate-reducing bacteria (Stroes-Gascoyne and West, 1997) results in sulphide production which may cause corrosion of steel or copper container materials. In addition, gas bubble production in the clay as a result of microbial respiration may create preferential pathways for gas and fluid migration (Moulin and Ouzounian, 1992; Nirex, 2006; Stroes-Gascoyne and West, 1997).

To date, there has been very little research on the characterization of NOM composition in bentonite clays (Hallbeck, 2010; Marshall and Simpson, 2014) and as such, it is difficult to predict whether or not NOM may serve as a microbial substrate in the DGR. Physical protection of NOM by clay minerals is thought to be one of the main mechanisms through which NOM persists in the environment (Schmidt et al., 2011). Therefore, it is possible that NOM on a clay surface will be protected from microbial degradation due to interactions such as ligand exchange and cation bridging with the clay surface (Feng and Simpson, 2011). Characterization of the structural composition of NOM in bentonite will foster a better understanding of the interactions between NOM and the clay surface including how this material is being protected by the clay surface.

Geochemical analysis was used to characterize five bentonite clay samples from deposits in Wyoming, Saskatchewan, India and Greece. The clays from Wyoming, Saskatchewan and India are all Na-rich bentonites while the clay from Greece is Ca-rich. Ca-rich clays were included for comparison to obtain a range of geochemical data to be used in limiting nutrients modelling and analysis and not necessarily because they are being considered as buffer material. Na-rich clays may be more desirable for the DGR because they tend to have lower hydraulic conductivities and higher swelling pressures than Ca-rich clays (Keto, 2003). NOM in the clays from Wyoming and Saskatchewan was characterized at the molecular-level using biomarker analysis and nuclear magnetic resonance (NMR) spectroscopy. These analyses were selected to allow the chemical structure of NOM, as well as its source and degradation state, to be evaluated (Baldock et al., 1992; Kögel-Knabner, 2000; Simpson et al., 2008). Biomarkers can be thought of as environmental tracers, which retain structural features of their parent precursor molecules and thus provide information about these precursor compounds (Simoneit, 2005). Gas chromatography coupled with mass spectrometry (GC-MS) is commonly employed for analysis of biomarkers. The use of GC-MS in tandem with solid-state ^{13}C and multi-dimensional solution-state ^{1}H NMR, allowed for a more complete characterization of NOM in these clays.

2. GEOCHEMICAL ANALYSIS

2.1 MATERIALS

Four sodium bentonites and one calcium bentonite were obtained. Two of the sodium bentonite samples are mined from the same deposit in Wyoming, USA: Volclay MX-80 (MX-80) by American Colloid Co. and National Standard Bentonite (National) by Opta Minerals Inc. Canadian Clay Products Inc. provided their Clay Products Sodium Bentonite (CCP) from the Bearpaw formation in Saskatchewan, Canada. The final sodium bentonite, Asha 505 (Asha), was from mined from a deposit in Kutch, India by Ashapura Minechem Co.. The calcium bentonite was mined from a deposit in Milos, Greece by S&B Industrial Minerals S.A. under the name IBECO RWC (RWC).

2.2 METHODS

All geochemical analyses were performed by the Soil and Nutrient Laboratory at the University of Guelph Laboratory Services in Guelph, Ontario, Canada. Brief descriptions of the methods used are provided below.

2.2.1 Carbon Analysis

Total carbon (C), inorganic carbon (IC) and organic carbon (OC) were determined using a LECO SC-444 element analyzer (Nelson and Sommers, 1982). Total C was determined using infrared detection to measure the amount of CO_2 evolved during combustion of the sample at 1350°C. Ashing of the sample at 475°C for three hours removed the OC and the procedure for total C determination was repeated on the ash sample to find the amount of IC. The IC result was subtracted from total C to determine OC. The MX-80 sample was sampled three different times and submitted for analysis to test reproducibility in a low OC sample and to determine sample heterogeneity. The average of replicate analysis had a standard error of <5%.

Water-extractable OC (WEOC) was isolated from clay samples by exhaustive extraction with Millipore water in preparation for solution-state ^{1}H NMR analysis of the MX-80, CCP and National samples. A ratio of 1:6 clay:water was used for MX-80 and CCP while a ratio of 1:12 clay:water was necessary for National due to differences in the water absorption capacity of the clays. The WEOC concentration was determined using a Shimadzu TOC-V_{CSH} total organic carbon (TOC) analysis with a high sensitivity combustion catalyst (720°C).

2.2.2 Nitrate and Nitrite

Samples were extracted with a 2 mol/L KCl solution to remove nitrate and nitrite. The resulting solution was treated with copperized cadmium to reduce nitrate to nitrite. A colour reagent was added after this reduction to form a reddish-purple azo dye which was measured at 520 nm using a Seal AQ2 spectrophotometer. The colour reagent is prepared by combining 800 mL deionized water, 100 mL phosphoric acid, 40 g sulfanilamide and 2 g N-(1-naphthyl)-ethylenediamine dihydrochloride and diluting to 1 L once the solids have dissolved. This was repeated without the reduction step to analyze for the nitrite that was originally present and the different between the two results was calculated to determine the nitrate concentration (O'Dell, 1993).

2.2.3 Inductive Coupled Plasma Optical Emission Spectrometry (ICP-OES) Analysis

K, Mg, Ca and Na were extracted from the clay by shaking in a 1 mol/L N ammonium acetate solution adjusted to pH 7 for 15 min (Simard, 1993), Fe was extracted from with a solution of 0.005 M pentetic acid (DPTA) and 2 h of shaking (Liang and Karamenos, 1993) and Mn was extracted with phosphoric acid (Reid, 1998). The resulting solutions were filtered and analyzed to determine the respective concentrations of the extracted species using a Varian ICP-OES.

2.2.4 Cation Exchange Capacity (CEC)

The cation exchange capacity (CEC) was determined by saturating the exchange sites in the clay samples with Ba^{2+} from a barium chloride solution. NH_4^+ was then used to displace the Ba^{2+} ions which can then be measured to quantify the CEC (Rhoades, 1982).

2.2.5 Heavy Metal Analysis

Clays (1 g) were combined with 3 mL concentrated HNO_3 and 9 mL concentrated HCl in digestion tubes and heated to 110°C on a heating block. This extraction does not dissolve silicates and thus metals bound to a silicate matrix were not measured. The extract was diluted with Nanopure water and analyzed using a Varian ICP-OES for Cd, Cr, Co, Cu, Mo, Ni, Pb and Zn (MOE, 2007). To extract Hg, the residue from the acid digestion was further digested with potassium permanganate and HCl and analyzed by cold vapour atomic absorption spectroscopy (AAS) (Russell and Pearce, 2009). Further digestion with potassium iodide and dilute HCl was required to extract As and further digestion with concentration HCl and heating was required for Se. Hydride generation AAS was used to analyze for Se and As (Pearce and Drouin, 2008).

2.2.6 Sulfur

Samples were microwaved in the presence of HNO_3 to extract S (Anderson, 1996) and the supernatant was diluted with Nanopure water before being analyzed using the Varian ICP-OES. The MX-80 sample was analyzed in replicate to test reproducibility of total sulphur analyses and to determine sample heterogeneity. The results of this test had a standard error of ca. ±5%.

2.2.7 pH

pH was determined by a saturated paste method in which clay samples were mixed with an appropriate amount of water to saturate the sample without any free-standing water. The resulting saturated paste was then measured with a pH meter.

2.2.8 Total Nitrogen

Samples were combusted in a sealed system at 800-1000°C to convert all forms of nitrogen to nitrogen oxides based on the Dumas method (Jung et al., 2003). The nitrogen compounds were reduced to N_2 gas and measured with a thermal conductivity cell in the LECO FP428.

2.2.9 Extractable Phosphorous

Phosphorous was extracted from samples using a 0.5 mol/L sodium bicarbonate solution (Reid, 1998) and the concentration was determined using a Seal AA3 spectrophotometer.

2.3 GEOCHEMICAL ANALYSIS RESULTS

The results of the geochemical analyses performed by the Soil and Nutrient Laboratory are summarized in Table 1. This data was collected to support limiting nutrient studies which requires a full suite of geochemical data. In addition to this, we also tested the sample heterogeneity using the MX-80 sample prior to analysis of the other samples. For three MX-80 subsamples, values of 0.721 ± 0.016%, 0.112 ± 0.0014%, 0.609 ± 0.018% for total C, OC, and IC were reported respectively. Total sulphur for the three replicates was reported at 0.38 ± 0.02%. This standard error was low and suggested that sample heterogeneity would not play a role in the geochemical analysis. As such, other analyses were not conducted in triplicate.

Table 1: Geochemical Characterization of Clay Samples

	MX-80	National	CCP	RWC	Asha
pH	8.3	9.0	7.9	8.1	8.6
CEC (cmol/kg)	76.3	64.0	48.3	71.3	73.5
Total S (%)	0.38[a]	0.22	0.11	0.30	0.13
Total N (%)	bdl	bdl	bdl	bdl	bdl
Extractable P (mg/kg)	4.6	20	14	2.7	3.4
Fe (mg/kg)	21	27.3	52	13.4	6.61
Nitrate (mg/kg)	2.91	7.31	49.8	2.33	1.94
Nitrite (mg/kg)	0.200	0.270	0.179	0.320	0.0396
Exchangeable Cations (mg/kg)					
Ca	4890	5590	2670	8880	7450
Mg	1700	700	410	3600	1900
K	560	490	530	570	190
Na	11856	11463	6843	4466	10863
Mn	2.29	2.19	19.4	5.43	2.90
Carbon (%)					
Total	0.721[a]	0.24	0.465	0.827	0.498
Organic	0.112[a]	0.24	0.414	0.083	0.149
Inorganic	0.609[a]	bdl	0.0513	0.744	0.349
Water-extractable organic	0.0095	0.016	0.073	n/a	n/a
Trace Metals (ug/g)					
As	5.3	9.2	6.4	4.1	<0.35
Se	0.13	0.16	0.32	0.50	0.11
Co	1.6	0.86	5.6	5.4	61
Cr	4.5	1.9	19	11	140
Cd	<0.2	<0.2	<0.2	<0.2	<0.2
Cu	3.2	2.9	15	19	150
Hg	<0.035	<0.035	0.055	0.26	<0.035
Mo	2.4	2.7	0.098	1.1	<0.7
Ni	7.8	2.9	17	5.5	77
Pb	43	43	20	9.8	9.5
Zn	55	71	66	23	200

bdl = below detectable limits (<0.05); [a]Represent average values of triplicate analysis (see section 2.3 for more information); n/a = not applicable because these samples were not extracted for ^{1}H NMR spectroscopy (see section 3 for more information).

Analysis of clay samples from these deposits has also been conducted in other studies, as noted below (see Table 2). The CCP and National samples were not analyzed in any of the other studies reviewed and thus there are only results for the MX-80, RWC and Asha samples. Parameters that were found in multiple studies are presented as ranges.

Table 2: Comparison of Geochemical Literature Values

	MX-80	RWC	Asha
CEC (cmol/kg)	75-86.3[a,c-e]	72-100[a-3]	88.6-93.3[d,3]
Exchangeable Cations (mg/kg)			
Ca	5210-13627[a,c-e]	11823-38475[b-3]	-
Mg	1142-2187 [a,c-e]	4193-7293[b-3]	-
K	391-782 [a,c-e]	508-997[b-3]	391[c]
Na	11725-13449 [a,c-e]	3104-5134[b-e]	13564[c]
Carbon (%)			
Total	0.398[a]	1.14-1.78[a,b]	-
Organic	0.15-0.235[a,e]	0.07-0.22[a,e]	-
Inorganic	0.15-0.163[a,e]	0.92-1.24[a,e]	-

[a]Karnland (2010); [b]Olsson and Karnland (2009); [c]Kumpulainen and Kiviranta (2010); [d]Svensson et al. (2011); [e]Kiviranata and Kumpulainen (2011).

2.4 DISCUSSION OF GEOCHEMICAL ANALYSIS

As discussed previously, NOM in the buffer material may be a key nutrient source for microbes in the vicinity of the UFC (Oscarson et al., 1986). Thus, clay with a lower OC content and consequently a lower amount of NOM is preferred. All of the clays had low amounts of OC compared to other environmental samples but the MX-80, Asha and RWC clays had the least OC (Table 2). The WEOC in a sample is believed to be representative of the labile OC content (Simoneit et al., 2004). Less than 10% of the OC in samples MX-80 and National was water-extractable suggesting that there is very little labile material in these clay samples. Organic geochemical analyses (section 3) also provide insight into the composition of NOM and its potential to serve as a microbial substrate.

The MX-80 and National samples are mined from the same bentonite deposit in Wyoming. Similarities were observed between these samples but there some differences were also apparent. Most notably, the CEC values and carbon contents varied between the samples suggesting that there may be heterogeneity within the same clay deposit.

Compared to the literature values (Table 2), the values obtained for the CEC and exchangeable cations (Table 1) are consistent with other reports. The range of values reported for the clay samples also highlights variability within the clay deposits. The same result is observed when comparing calculated C values for the RWC clay with the literature. The IC result for the MX-80 clay was much higher than the literature values while the OC result was slightly below the literature range. As such, it is important to monitor basic geochemistry with each deposit because of the inherent variability of the clay samples.

3. MOLECULAR-LEVEL ANALYSIS OF NATURAL ORGANIC MATTER IN CLAY SAMPLES

3.1 MATERIALS

Three candidate clay samples were chosen for detailed NOM molecular-level analysis. The two clays from the Wyoming, USA deposit, MX-80 and National, were analyzed as well as CCP from

Saskatchewan, Canada. These clays represent the range of OC and CEC found through the geochemical analysis. MX-80 is also the current reference clay for the NWMO repository design (Villagran et al., 2011). All five clays were prepared for solid-state ^{13}C NMR analysis for detailed comparisons.

3.2 METHODS

3.2.1 Chemical Extractions and GC-MS Analysis

MX-80, National and CCP clay samples were subjected to a series of chemical extractions to isolate NOM biomarkers that can provide information about the source and degradation stage of NOM. Biomarker analyses included: solvent-extractable lipids and other unbound compounds; base hydrolysis to isolate bound (hydrolysable) lipids; and CuO oxidation to isolate lignin-derived phenols (Otto and Simpson, 2005; Otto and Simpson, 2006a; Otto and Simpson, 2006b). Specifically, a 90 g sample of each clay was sonicated sequentially in dichloromethane, a mixture of dichloromethane and methanol (1:1 v/v), and methanol with 180 mL of each solvent. The resulting supernatant was filtered through glass fiber filters (Whatman GF/A and GF/F), concentrated by rotary evaporation and dried under N_2 flow. Air-dried clay residues from the solvent extraction (8 g) were transferred to Teflon liners and heated at 100°C for 3 h in metal reaction bombs in the presence of 20 mL of 1 M methanolic KOH. The resulting extracts were acidified to pH 1 with 6M HCl and hydrolysable lipids were separated by liquid-liquid extraction with diethyl ether followed by rotary evaporation to remove diethyl ether. Residues from the base hydrolysis (8 g) were air-dried for isolation of lignin-derived phenols with 1 g of copper (II) oxide [CuO], 100 mg ammonium (II) iron sulfate hexahydrate [$Fe(NH_4)_2(SO_4)_2 \cdot 6H_2O$] and 15 mL of 2 M NaOH heated at 170°C for 2.5 h. After acidification to pH 1 with 6 M HCl, extracts were stored for 1 h at room temperature in the dark to prevent reactions of cinnamic acids. Extract solutions were then centrifuged and lignin-derived phenols were liquid-liquid extracted from the supernatant with diethyl ether. Rotary evaporation was used to remove diethyl ether.

Base hydrolysis extracts were derivatized with *N,N*-Dimethylformamide dimethyl acetal (methyl-8) at 60°C for 30 min. The solvent extract, CuO oxidation extract and the derivatized base hydrolysis extract were derivatized using *N,O*-bis-(trimthylsilyl)trifluoroacetamide (BSTFA) and pyridine at 70°C for 1.5 h. Derivatized compounds were transferred to 250 µL vial inserts with hexane and injected into an Agilent model 6890N gas chromatograph coupled to an Agilent model 5973 quadrupole mass selective detector using an Agilent model 7683 autosampler. Separation by gas chromatography (GC) was achieved with an HP-5MS fused silica capillary column (30 m x 0.25 mm inner diameter x 0.25 µm film thickness). GC operating conditions were as follows: initial temperature of 65°C held for 2 min, temperature increase from 65°C to 300°C at a rate of 6°C per min and a final temperature of 300°C held for 20 min. Compounds were identified by comparison with mass spectra in the Wiley275 MS library. Tetracosane, methyl tricosanoate and behenyl alcohol-TMS were used as external quantification standards for the solvent extracts while methyl tricosanoate was used for the hydrolysable lipids and vanillic acid-TMS was used for lignin-derived phenols. All extractions were performed in triplicate.

3.2.2 Detection and Quantification Limits

Due to the low concentrations observed for the biomarker compounds, the detection and quantification limits of the GC-MS were tested. The standards used in the quantification of the biomarker extracts (tetracosane, methyl tricosanoate, behenyl alcohol and vanillic acid) were used to test the limit of detection (LOD) and limit of quantification (LOQ) for *n*-alkanes, *n*-alkanoic acids, *n*-alkanols and phenols. Standards ranging from 10-100 mg/L were analyzed using the same procedure as the analysis of the biomarker extracts. Standards in the concentration range 100-1000 mg/L were also analyzed to ensure a linear response. The signal-to-noise ratio (S/N) was determined by measuring the heights of the signal peak and noise region. The LOD and LOQ are defined as S/N≥3 and S/N=10 respectively (Dass, 2007).

3.2.3 Solid-State ^{13}C NMR

All five clay samples (100 g) were repeatedly treated with a solution of 10% HF acid and 4% HCl acid to enrich the organic matter and remove paramagnetic ions that can interfere with NMR analysis (Gonclaves et al. 2003; Rumpel et al. 2006; Schmidt et al. 1997). After treatment, samples were washed with deionized water and freeze-dried. Treated clays (100 mg) were packed into 4 mm zirconium rotors with Kel-F caps for analysis by solid-state ^{13}C cross polarization magic angle spinning (CPMAS) NMR. Spectra were acquired on a 500 MHz Bruker BioSpin Avance III spectrometer with a 4 mm H-X MAS probe. A ramp-CP pulse program (Conte et al., 2004) was used with a spinning rate of 13 kHz, a contact time of 1 ms and a 3 s recycle delay. Preliminary experiments were performed to optimize the recycle delay and ensure that it was longer than four times the spin-lattice relaxation of protons within the sample. NMR spectra were processed with TopSpin version 3.0 using a zero-filling factor of 2 and 100 Hz line broadening. Four spectral regions were integrated: alkyl, 0-50 ppm; *O*-alkyl, 50-110 ppm; aromatic + phenolic, 110-165 ppm; and carboxylic + carbonyl, 165-220 ppm (Baldock et al., 1992; Preston et al., 1997; Simpson et al., 2008).

3.2.4 Solution-State NMR

Both water-soluble and base-soluble (humic substances) NOM was extracted and analyzed by solution-state NMR spectroscopy. Water-soluble NOM was isolated from the three clay samples used in the biomarker analysis by exhaustive extraction with Millipore water as described in section 2.2.1. The extract was centrifuged at 30,000*g* for 1 h to remove suspended clay particles and freeze-dried. HF and HCl treated samples were exhaustively extracted with 0.1 M NaOH under N_2 to extract base-soluble NOM (humic substances). Extracts were filtered through a 0.22 µm Millipore Durapore PVDF membrane filter, passed through an Amberjet 1200(H) ion exchange resin for cation exchange and freeze-dried. Base-soluble extracts (5 mg) were dried further over phosphorous pentoxide [P_2O_5] before being dissolved in 60µL of DMSO-d_6 and transferred to a 1.7 mm NMR tube. A 15 mg sample of the water extraction residue was mixed with 80 µL of deuterium oxide (D_2O, 99.96% D) and adjusted to pH 12 by addition of 5 µL sodium deuteroxide (NaOD, 99.5% D, 30% in D_2O). The mixture was vortexed for 2 min, centrifuged at 2300*g* for 20 minutes and 30 µL of supernatant was transferred to a 1.7 mm NMR tube. The water- and base-solution fractions were analyzed with one-dimensional (1D) solution-state ^1H NMR. Two-dimensional (2D) solution-state ^1H NMR spectra were obtained for the base-soluble NOM extracted from the CCP clay sample to confirm the peak assignments made in the 1D spectra. The CCP sample was chosen for 2D analysis because it has the highest OC content and gave the highest NMR response.

Solution-state ^{1}H NMR spectra were acquired using a Bruker BioSpin Avance III 500 MHz spectrometer with a ^{1}H-^{13}C-^{15}N 1.7 mm microprobe fitted with an actively shielded Z-gradient at 298K. Presaturation utilizing relaxation gradients and echoes (PURGE) was used to suppress the water signal at 4.7 ppm (Simpson and Brown, 2005). 1D NMR spectra were collected using 2K scans, a recycle delay of 1 s and 32,768 time delay points. Spectra were processed with TopSpin 3.0 software using a zero filling factor of 2 and 1 Hz line broadening. Peaks were assigned using the additional information provided by the 2D solution-state ^{1}H NMR experiments and the literature (Deshmukh et al., 2003; Simpson et al., 2003). 2D spectra were collected as follows.

Correlation spectroscopy (COSY) data were acquired using digital quadrature detection with 2048 scans, a spectral width of 7500 Hz and 196 time domain increments. Spectra were processed using a QSINE function and magnitude mode for the F1 axis, a zero-filling factor of 2 and 1 Hz line broadening. Total correlation spectroscopy (TOCSY) data were acquired in the phase-sensitive mode with a mixing time of 80 ms. A total of 2048 scans were collected for each of the 196 increments in the F1 axis and 2048 data points were collected for the F2 axis Heteronuclear single quantum coherence (HSQC) data were obtained using digital quadrature detection with anti-echo gradient selection and an average ^{1}J ^{1}H-^{13}C value of 145 Hz. A total of 2048 scans were collected in the F1 axis for each of the 128 increments and 2048 data points were collected for the F2 axis. Both TOCSY and HSQC spectra were processed with a function corresponding to 15 Hz for the F2 axis and an unshifted sine-squared function for the F1 axis. A zero-filling factor of 2 was used for both axes.

3.3 RESULTS OF NOM MOLECULAR LEVEL ANALYSIS

3.3.1 Chemical Extractions and GC-MS Analysis

The LOD and LOQ values determined by the quality control tests are shown in Table 3.

Table 3: GC-MS Detection Limits for Representative Biomarker Compounds

Compound	Amount (ng)	S/N
Behenyl alcohol		
LOD	25	6.3
LOQ	35	11.0
Tetracosane		
LOD	10	4.0
LOQ	25	9.0
Methyl tricosanoate		
LOD	25	4.1
LOQ	60	10.9
Vanillic acid		
LOD	10	4.1
LOQ	15	9.3

The results of the solvent extraction of the MX-80, CCP and National clay samples are listed in Table 4. Due to sample heterogeneity and low NOM concentration, some compounds were only observed in one or two replicates as indicated by the superscripts. In general, a variety *n*-alkanoic acids, *n*-alkanols and *n*-alkanes were observed. The sources of these compounds as well as some commonly used *n*-alkane proxies are also indicated in the table.

Table 4: Major Components of NOM (ng/g Clay) and Their Sources Identified After Solvent Extraction of MX-80, National and CCP Clays

	MX-80	National	CCP	Source
n-Alkanoic acids				
Short chain				
Hexanoic acid	7.71[a]	26.7 ± 7.63	bdl	
Heptanoic acid	2.16[a]	4.26 ± 0.41	bdl	
Octanoic acid	6.46[b] ± 5.33	9.03 ± 4.46	2.49[b] ± 0.20	
Nonanoic acid	bdl	10.5 ± 4.31	bdl	
Decanoic acid	4.32[a]	4.22 ± 1.53	1.98[b] ± 0.31	
Undecanoic acid	2.38[b] ± 0.11	5.61 ± 1.65	1.45 ± 0.41	
Dodecanoic acid	1.67[b] ± 0.63	11.4 ± 4.60	4.56 ± 1.37	
Tridecanoic acid	2.94[b] ± 0.89	8.73 ± 2.18	8.92 ± 2.46	Microbes, plants and mosses[c,d,e]
Tetradecanoic acid	8.42[b] ± 1.36	26.5 ± 9.72	21.2 ± 3.99	
Pentadecanoic acid	bdl	15.8 ± 3.22	27.4 ± 7.48	
Hexadecanoic acid	113[b] ± 45.9	242 ± 67.7	128 ± 13.1	
Heptadecanoic acid	2.76[b] ± 2.69	16.4 ± 7.49	39.9 ± 4.63	
cis-9-Octadecenoic acid	bdl	140 ± 69.4	35.4 ± 5.49	
Octadecanoic acid	151 ± 109	482 ± 98.9	151[b] ± 16.38	
Nonadecanoic acid	2.47[b] ± 0.26	10.9 ± 4.09	34.4 ± 6.66	
Long-chain				
Eicosanoic acid	bdl	bdl	39.0 ± 8.99	
Heneicosanoic acid	bdl	15.3 ± 5.06	40.3[b] ± 4.52	
Docosanoic acid	8.60[b] ± 1.40	20.8 ± 7.60	30.8 ± 8.10	
Tricosanoic acid	5.06[b] ± 1.49	22.4 ± 6.47	24.1 ± 6.91	
Tetracosanoic acid	9.44 ± 3.18	bdl	23.3 ± 7.60	Vascular plant waxes[f]
Pentacosanoic acid	bdl	16.8[b] ± 10.3	10.7 ± 4.03	
Hexacosanoic acid	6.76[b] ± 0.95	23.9[b] ± 16.0	21.4 ± 8.49	
Heptacosanoic acid	bdl	-	9.32[b] ± 1.59	
Octacosanoic acid	bdl	30.4[b] ± 13.1	24.9 ± 6.53	

Table 4: Continued

	MX-80	National	CCP	Source
n-Alkanols				
Short chain				
Dodecanol	2.27 ± 1.26	2.75 ± 1.20	5.61[b] ± 0.58	Microbes[b,g]
Tridecanol	1.24[a]	3.32 ± 0.91	6.70 ± 2.85	
Tetradecanol	bdl	1.23[b] ± 0.0025	3.64[b] ± 0.35	
Pentadecanol	bdl	0.20[a]	2.26 ± 0.65	
Hexadecanol	bdl	0.59[b] ± 0.18	bdl	
Octadecanol	bdl	0.79[b] ± 0.070	3.37[b] ± 0.18	
Long-chain				
Icosanol	2.62 ± 1.00	8.42 ± 2.21	bdl	Vascular plant waxes[f]
Docosanol	5.58[b] ±0.96	bdl	bdl	
Tetracosanol	4.11[b] ± 1.70	13.4 ± 4.68	5.72[b] ± 1.11	
Hexacosanol	bdl	4.56[b] ± 1.53	4.79 ± 1.22	
Octacosanol	2.28[b] ± 0.016	bdl	3.72[b] ± 0.23	
n-Alkanes				
Short chain				
Octadecane	bdl	6.60 ± 0.92	13.2[b] ± 0.84	Plants or microbes[d,e]
Nonadecane	4.53[b] ± 2.07	5.63 ± 0.80	8.12[b] ± 2.01	
Long-chain				
Icosane	5.09 ± 2.63	16.6 ± 1.65	11.5 ± 4.63	Vascular plant waxes[f]
Heneicosane	5.64 ± 2.28	14.8 ± 1.16	16.2[b] ± 0.93	
Docosane	4.08[b] ± 0.077	19.9 ± 5.00	8.22[b] ± 3.13	
Tricosane	8.14 ± 4.36	6.61 ± 1.01	18.7 ± 4.09	
Tetracosane	10.3[b] ± 1.23	29.3[b] ± 4.50	bdl	
Pentacosane	5.37 ± 1.91	12.8[b] ± 5.93	30.1 ± 6.91	
Hexacosane	6.59[b] ± 3.99	14.9 ± 2.60	14.2 ± 3.88	
Heptacosane	13.1 ± 4.03	23.1 ± 2.56	41.1 ± 8.96	
Octacosane	11.1 ± 4.92	bdl	64.7 ± 26.6	
Nonacosane	14.3 ± 4.84	bdl	bdl	
Triacontane	bdl	13.8 ± 1.69	9.59 ± 2.31	
Hentriacontane	8.62 ± 3.94	37.7 ± 11.5	38.8 ± 11.9	
Tritriacontane	bdl	10.8 ± 1.53	20.1[b] ± 0.77	
n-Alkane proxies				
$C_{23}/(C_{23}+C_{27})$	0.32	0.22	0.31	
$C_{31}/(C_{27}+C_{31})$	0.37	0.60	0.47	
$C_{29}/(C_{27}+C_{29}+C_{31})$	0.40	bdl	bdl	

bdl = below detection limits, [a] = compound identified in only one of three replicates (no SE calculated, the single high measurement is reported), [b] = compound identified in two of three replicates (SE of the two detected measurements is reported); [c] Baas et al. (2000); [d] Harwood and Russel (1984); [e] Volkman et al. (1998); [f] Bianchi (1995); [g] Ficken et al. (2000).

Table 5 lists the results of the second extraction method applied to the three clay samples, base hydrolysis. As with the solvent extraction, some of the compounds observed in this extract were not observed in all three replicates. There were also some samples that had concentration values near the LOD, denoted as ‘Tr’ or trace amounts, and others that had values between the LOD and LOQ which are denoted as ‘Det’ or detected. The compounds extracted included *n*-alkanoic acids, *α*-hydroxyalkanoic acids, *ω*-hydroxyalkanoic acids, *α,ω*-alkanedioic acids and *p*-hydroxybenzoic acid.

Table 5: Major Components of NOM (ng/g Clay) and Their Sources Identified After Base Hydrolysis of MX-80, National and CCP Clays

	MX-80	National	CCP	Source
Short chain n-alkanoic acids				
Nonanoic acid	bdl	bdl	173[a]	
Dodecanoic acid	Det[a]	Tr[a]	38.9[b] ± 26.9	
Tridecanoic acid	bdl	bdl	21.9[a]	
Tetradecanoic acid	55.2 ± 4.45	27.0 ± 13.9	73.3 ± 46.2	
Pentadecanoic acid	bdl	17.2[a]	38.7 ± 20.1	Microbes and plants[d,e]
Hexadecanoic acid	675 ± 318	698[b] ± 261	1409[b] ± 1120	
Heptadecanoic acid	Det[a]	Det[a]	60.7 ± 24.6	
Octadecanoic acid	1085 ± 496	1327 ± 436	2612 ± 1442	
trans-9-Octadecenoic acid	bdl	34.1[a]	bdl	
cis-9-Octadecenoic acid	682 ± 19.2	25.4[b] ± 7.82	84.2[b] ± 22.3	
Long-chain n-alkanoic acids				
Nonadecanoic acid	bdl	bdl	36.0 ± 21.5	
Eicosanoic acid	27.6[b] ± 13.2	50.0[a]	79.0 ± 45.4	
Docosanoic acid	bdl	bdl	74.5[a]	Vascular plant waxes and suberin[f]
Tricosanoic acid	bdl	bdl	16.4[a]	
Tetracosanoic acid	bdl	bdl	59.5[a]	
Hexacosanoic acid	bdl	bdl	18.5[a]	
Triacontanoic acid	bdl	bdl	43.9[a]	
α-Hydroxyalkanoic acids				
α-Hydroxytridecanoic acid	bdl	23.6[a]	Det[a]	
α-Hydroxypentadecanoic acid	bdl	44.0[a]	43.9[b] ± 37.2	
α-Hydroxyhexadecanoic acid	30.2 ± 4.49	27.3[b] ± 4.99	56.6[a]	Leaf waxes and wood[g]
α-Hydroxyheptadecanoic acid	bdl	Det[a]	23.9[b] ± 16.0	
α-Hydroxyoctadecanoic acid	bdl	bdl	42.2[a]	
α,ω-Alkanedioic acids				
α,ω-Nonanedioic acid	bdl	116[a]	54.6 ± 43.7	
α,ω-Decanedioic acid	bdl	bdl	26.6[b] ± 21.0	
α,ω-Undecanedioic acid	bdl	bdl	26.3 ± 13.8	Suberin[h]
α,ω-Nonadecanedioic acid	bdl	bdl	84.3[a]	
α,ω-Eicosanedioic acid	bdl	bdl	37.9[a]	
ω-Hydroxyalkanoic acids				
ω-Hydroxyundecanoic acid	bdl	35.2[a]	bdl	
ω-Hydroxydodecanoic acid	bdl	27.9[a]	bdl	Suberin[h]
ω-Hydroxyoctadecanoic acid	bdl	172[a]	bdl	
Other products				
p-Hydroxybenzoic acid	bdl	bdl	25.6[a]	Lignin or proteins[i]

Tr = trace amounts of compound (at LOD), Det= compound detected but not quantifiable (below LOQ), bdl = below detection limits, [a] = compound identified in one of three replicates (no SE calculated, the single high measurement is reported), [b] = compound identified in two of three replicates (of the two detected measurements is reported); [d] Harwood and Russel, (1984); [e] Volkman et al. (1998); [f] Otto and Simpson (2006b); [g] Friere et al. (2002); [h] Kolattukudy and Espelie, (1989); [i] Goñi et al. (2000).

CuO oxidation results are shown in Table 6. As with the base hydrolysis, some of the concentrations were below the LOD and LOQ values determined by the quality control tests (section 3.3.1). Sample heterogeneity was also observed in replicates of this extraction. CuO oxidation normally yields vanillyl (vanillin, acetovanillone and vanillic acid), syringyl (syringaldehyde, acetosyingone and syringic acid) and cinnamyl (*p*-coumaric acid and ferulic acid) groups (Hedges and Mann, 1979). Vanillin was detected in the extract from the National clay while vanillic acid was detected in extracts from all three samples. *n*-Alkanoic acids, *α,ω*-Alkanedioic acids, *m*- and *p*-hydroxybenzoic acid, 3,5-dihyroxybenzoic acid and 1,4-benzenedicarboxylic acid were also detected.

Table 6: Major Components of NOM (ng/g Clay) and Their Sources After CuO Oxidation of MX-80, National and CCP Clays

	MX-80	National	CCP	Source
n-Alkanoic acids				
Octanoic acid	Det[a]	bdl	bdl	
Nonanoic acid	11.4[b] ± 9.83	18.4[a]	40.5[a]	
Decanoic acid	Det[a]	Det[b]	9.2[a]	
Dodecanoic acid	Tr[b]	bdl	9.5 ± 2.53	
Tetradecanoic acid	Det[a]	Det[b]	13.4 ± 1.42	Microbes and plants[c,d]
Pentadecanoic acid	Tr[a]	Tr[a]	Det[b]	
Hexadecanoic acid	45.3[a]	53.8[a]	309 ± 131	
Heptadecanoic acid	bdl	bdl	Det[b]	
cis-9-Octadecenoic acid	bdl	Tr[a]	10.1[a]	
Octadecanoic acid	55.8[a]	115[a]	393 ± 189	
α,ω-Alkanedioic acids				
α,ω-Heptanedioic acid	bdl	bdl	16.3[a]	Suberin[e]
α,ω-Nonanedioic acid	20.2[b] ± 10.3	16.6[b] ± 8.32	37.2 ± 9.56	
Protein-derived products				
m-Hydroxybenzoic acid	8.3[b] ± 0.76	bdl	15.8 ± 4.29	Plant-derived proteins[f]
p-Hydroxybenzoic acid	11.6[b] ± 3.12	bdl	20.4 ± 4.14	
Other benzenes				
3,5-Dihydroxybenzoic acid	bdl	bdl	56.9[b] ± 22.8	Tannins[g]
1,4-Benzenedicarboxylic acid	bdl	bdl	2.6[a]	
Lignin monomers				
Vanillin	bdl	290[b] ± 73.5	bdl	Gymnosperm wood[h]
Vanillic acid	11.07[b] ± 0.74	1491[a]	232[b] ± 58.5	

Tr= trace amounts of compound (at LOD), Det= compound detected but not quantifiable (below LOQ), bdl = below detection limits, [a] = compound identified in one of three replicates (no SE calculated, the single high measurement is reported), [b] = compound identified in two of three replicates (SE of the two detected measurements is reported); [c] Harwood and Russel (1984); [d] Volkman et al. (1998); [e] Kolattukudy and Espelie (1989); [f] Goñi et al. (2000); [g] Prahl et al. (2004); [h] Hedges and Mann (1979).

3.3.2 Solid-State ^{13}C NMR

^{13}C NMR spectra were successfully collected for the MX-80, CCP and National samples. Despite extensive sample pre-treatment, no signal was observed for the Asha or RWC samples after 48 hours of analysis (signal is usually obtained within 1-2 hours for pre-treated samples). The spectra that were collected are shown in Figure 2. The four main spectral regions identified correspond to aliphatic carbon, 0-50 ppm; *O*-alkyl carbon, 50-110 ppm; aromatic and phenolic carbons, 110-165 ppm; and carboxyl and carbonyl carbons, 165-220 ppm (Baldock et al., 1992; Simpson et al., 2008).

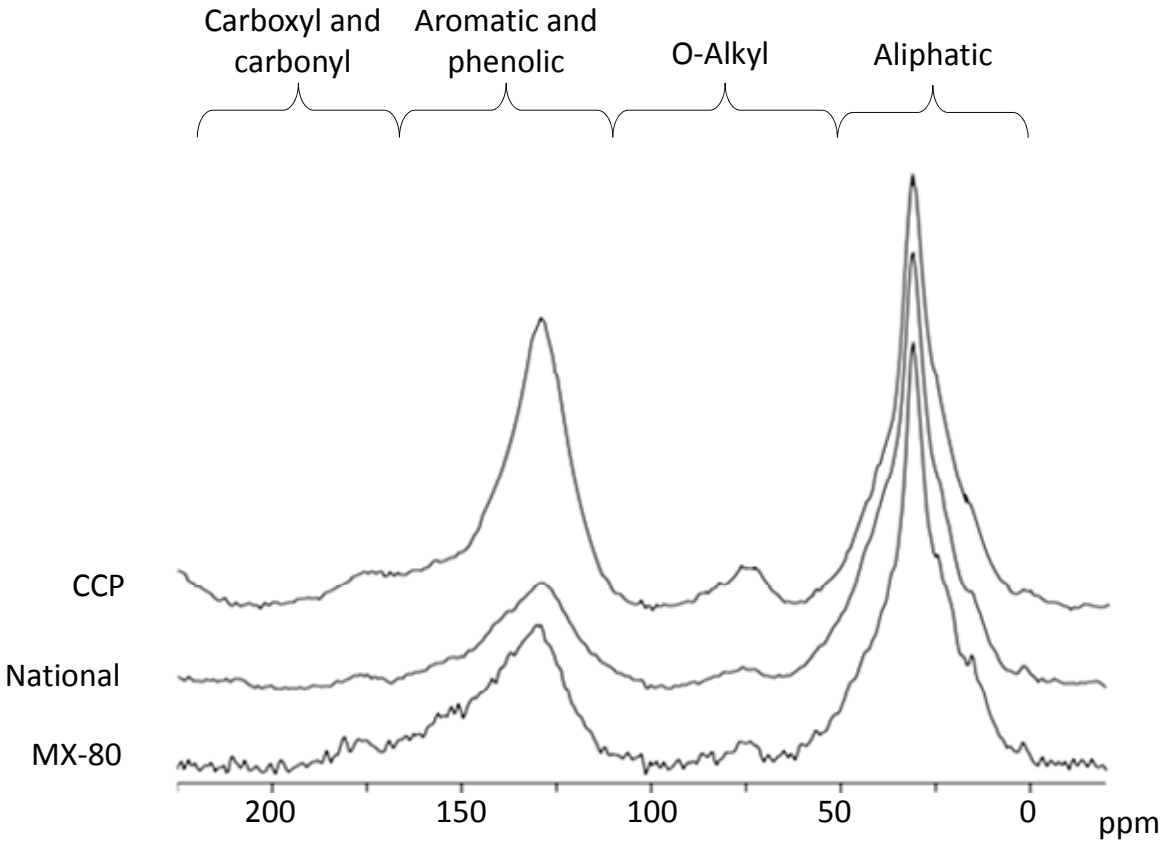

Figure 2: Solid-State CPMAS ^{13}C NMR Spectra of HF-Treated Clay Samples from Wyoming, USA and Saskatchewan, Canada showing the four major spectral regions: aliphatic, 0-50 ppm; *O*-alkyl, 20-110 ppm; aromatic & phenolic, 110-165 ppm and carboxyl & carbonyl, 165-220 ppm (Baldock et al., 1992; Simpson et al., 2008).

The relative abundance (%) of integrated signal area found in each of these regions is reported in Table 7. The aliphatic and the aromatic and phenolic regions contained the highest amount of signal in the case of all three clays. Possible sources of this material are also listed. To further establish the potential source of the NOM, solution-state NMR was performed on the soluble (water extractable and base extractable) portion of the NOM (see section 3.3.3).

Table 7: Relative Abundance (%) of Solid-State ^{13}C NMR Signal for Different Structural components of NOM

Structural region	Chemical shift (ppm)	MX-80	National	CCP	Source
Aliphatic	0 - 50	56	68	46	Aliphatic compounds found in lipids, waxes, cutin and suberin[a,b]
O-Alkyl	50 - 110	7	7	6	Substituted aliphatic compounds found in carbohydrates, proteins, and lignin[b]
Aromatic and phenolic	110 - 165	32	24	42	Aromatic components found in lignin, proteins and black carbon[b,c]
Carboxyl and carbonyl	165 - 220	5	1	6	Carboxylic, amide and ester carbons found in NOM[b]

[a] Preston et al. (1997); [b] Simpson et al. (2008); [c] Baldock et al. (1992).

3.3.3 Solution-State ^{1}H NMR

The results of the 1D NMR analyses of the water- and base-soluble extracts were evaluated with the results of the 2D analysis of the base-soluble material to make structural assignments for the spectra based on previously published literature assignments for NOM (Deshmukh et al., 2003; Simpson et al., 2003). Peak assignments were made corresponding to carbons and protons in molecules similar to those shown in Table 8. These include: A, terminal methyls and main-chain methylenes; B, methylenes attached to COOH; C, methylenes in free primary alcohols; D, methylenes in free secondary alcohols and E, protons α to C-O including primary and secondary alcohols, ether, esters and carbohydrates.

Table 8: Carbon and Proton Pairs Identified in Clay Sample CCP and Corresponding Chemical Shifts (Deshmukh et al., 2003; Simpson et al., 2003).

Symbol	Type	^{1}H shift (ppm)	^{13}C shift (ppm)
A_1	$\underline{CH_3}$-CH_2-CH_2-R	0.7	14
A_2	CH_3-$\underline{CH_2}$-CH_2-R	0.9	20
A_3	CH_3-CH_2-$\underline{CH_2}$-R	1.1	29
B_1	R-CH_2-$\underline{CH_2}$-CO_2H	2.0	34
B_2	R-$\underline{CH_2}$-CH_2-CO_2H	1.3	25
C_1	R-CH_2-$\underline{CH_2}$-CH_2-OH	1.4	35
C_2	R-$\underline{CH_2}$-CH_2-CH_2-OH	1.3	25
D_1	R-CH_2-$\underline{CH_2}$-CHOH-CH_2-CH_2-R	1.4	35
D_2	R-$\underline{CH_2}$-CH_2-CHOH-CH_2-CH_2-R	1.3	25
E	Protons α to C-O	3-3.8	58-74

Figure 3 shows the 1D spectrum of the base-soluble material extracted from clay sample CCP. This spectrum was chosen because it is representative of the spectra obtained for the MX-80 and National samples but has a higher signal intensity and better resolution. Spectral regions were assigned based on the literature and correspond to: aliphatic protons from methyl and methylene (0.3-2.9 ppm), *O*-alkyl protons from carbohydrates and lignin (2.9-4.1 ppm), α^1H from proteins (4.1-4.8 ppm), aromatic protons from lignin and proteins (6.2-7.8 ppm) and amide protons from proteins (7.8-8.4 ppm) (Clemente et al., 2012). Most of the peaks were detected in the aliphatic and *O*-alkyl regions and correspond to protons identified in Table 8. The triplet at 7.05 ppm is consistent with ammonia (Clemente et al., 2012).

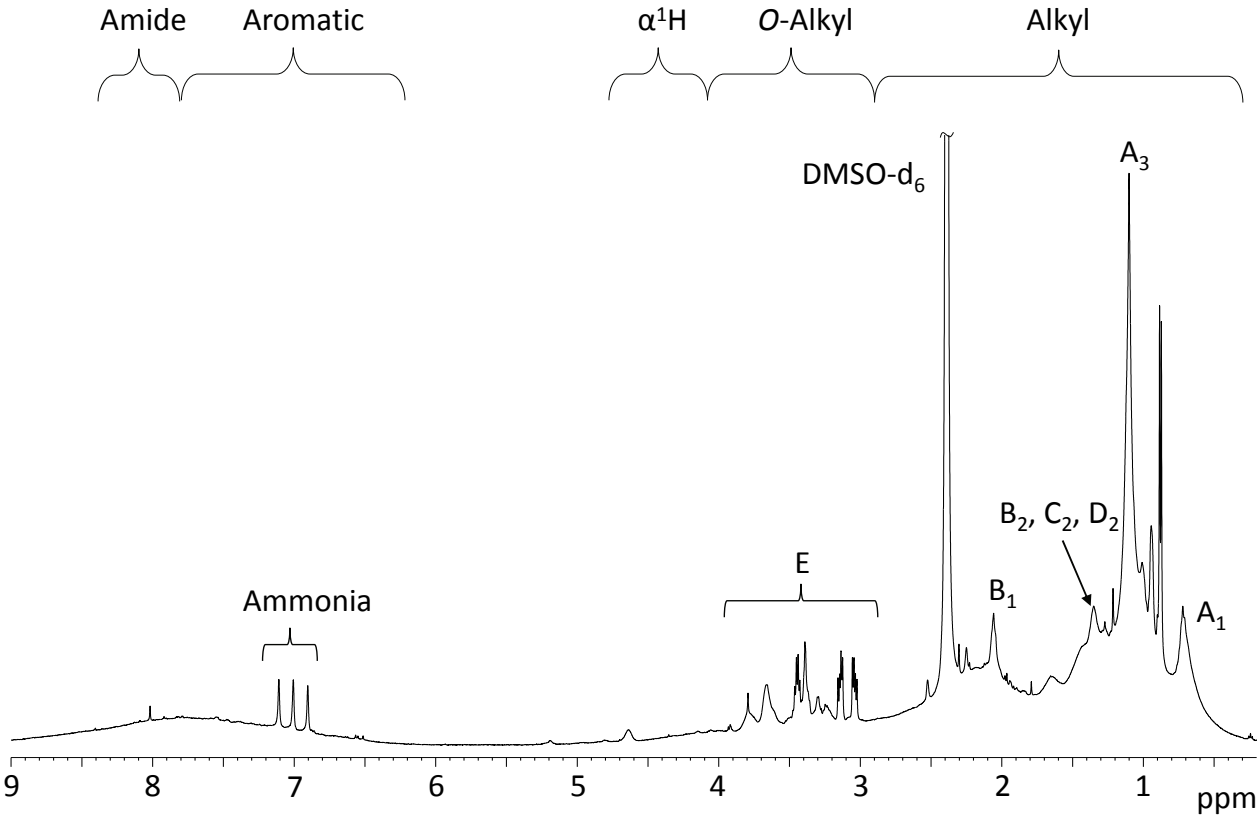

Figure 3: Solution-State ^{1}H NMR of the Base-Soluble Material Extracted from Clay Sample CCP. Highlighted Regions Correspond to the Following Protons: Aliphatic, 0.3-2.9 ppm; *O*-alkyl, 2.9-4.1 ppm; α^{1}H from proteins, 4.1-4.8 ppm; aromatic, 6.2-7.8 and amide, 7.8-8.4 (Clemente et al., 2012). Additional Peak Assignments (A_1, A_3, B_1, B_2, C_2, D_2 and E) are explained in Table 8.

The 1D spectrum representing the water-soluble extract for sample CCP also had a better signal intensity and resolution than the spectra from the other samples and thus is shown in Figure 4. This extract also mainly contains aliphatic and *O*-alkyl compounds that can be identified from Table 8. Some small organic molecules were also detected including formic acid (8.44 ppm), methanol (3.33 ppm) and acetic acid (1.90 ppm) (Woods et al., 2011).

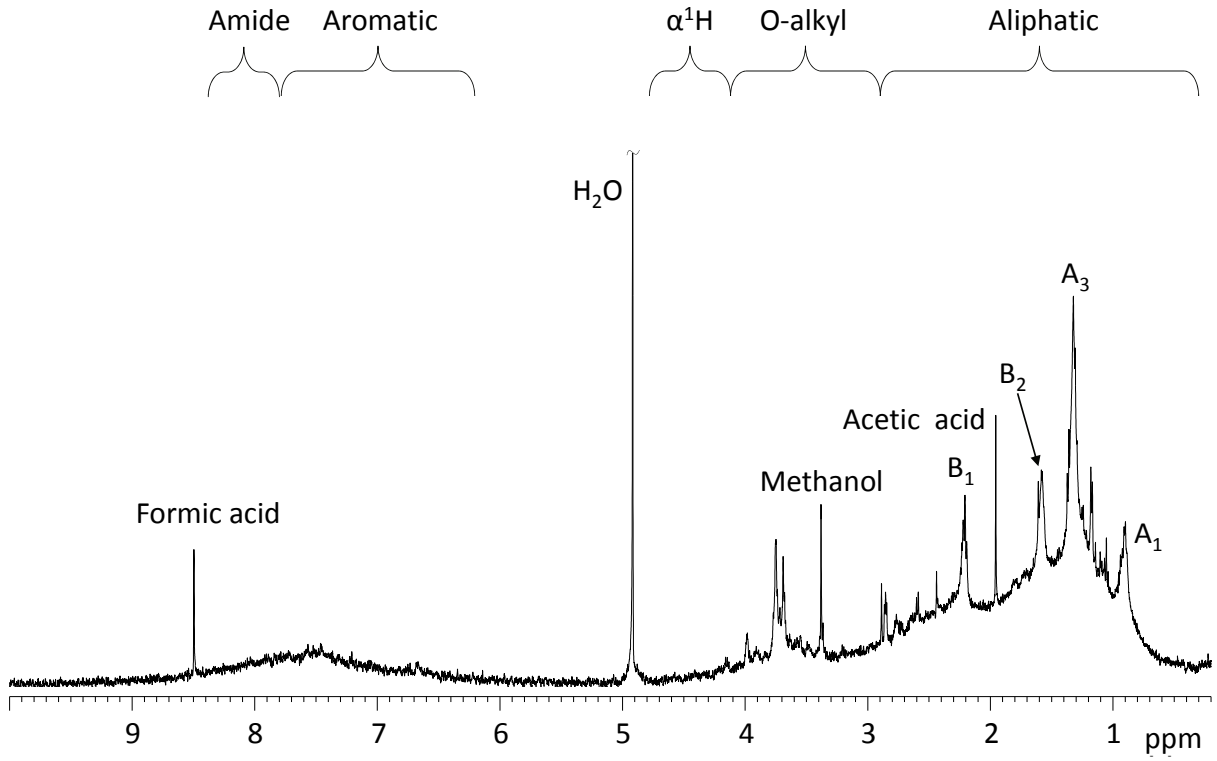

Figure 4: Solution-State ^{1}H NMR of the Water-Soluble Material Extracted from Clay Sample CCP. Highlighted Regions Correspond to the Following Protons: Aliphatic, 0.3-2.9 ppm; *O*-alkyl, 2.9-4.1 ppm; α^{1}H from proteins, 4.1-4.8 ppm; aromatic, 6.2-7.8 and amide, 7.8-8.4 (Clemente et al., 2012). Additonal peak assignments (A_1, A_3, B_1 and B_2) are explained in Table 8.

The final spectrum shown in Figure 5 is the 2D HSQC spectrum. COSY and TOCSY spectra were also obtained for this sample and were found to be consistent with the HSQC spectrum but are not shown for brevity. Peak assignments for this spectrum correspond to the couplings between the carbons and protons identified and listed in Table 8.

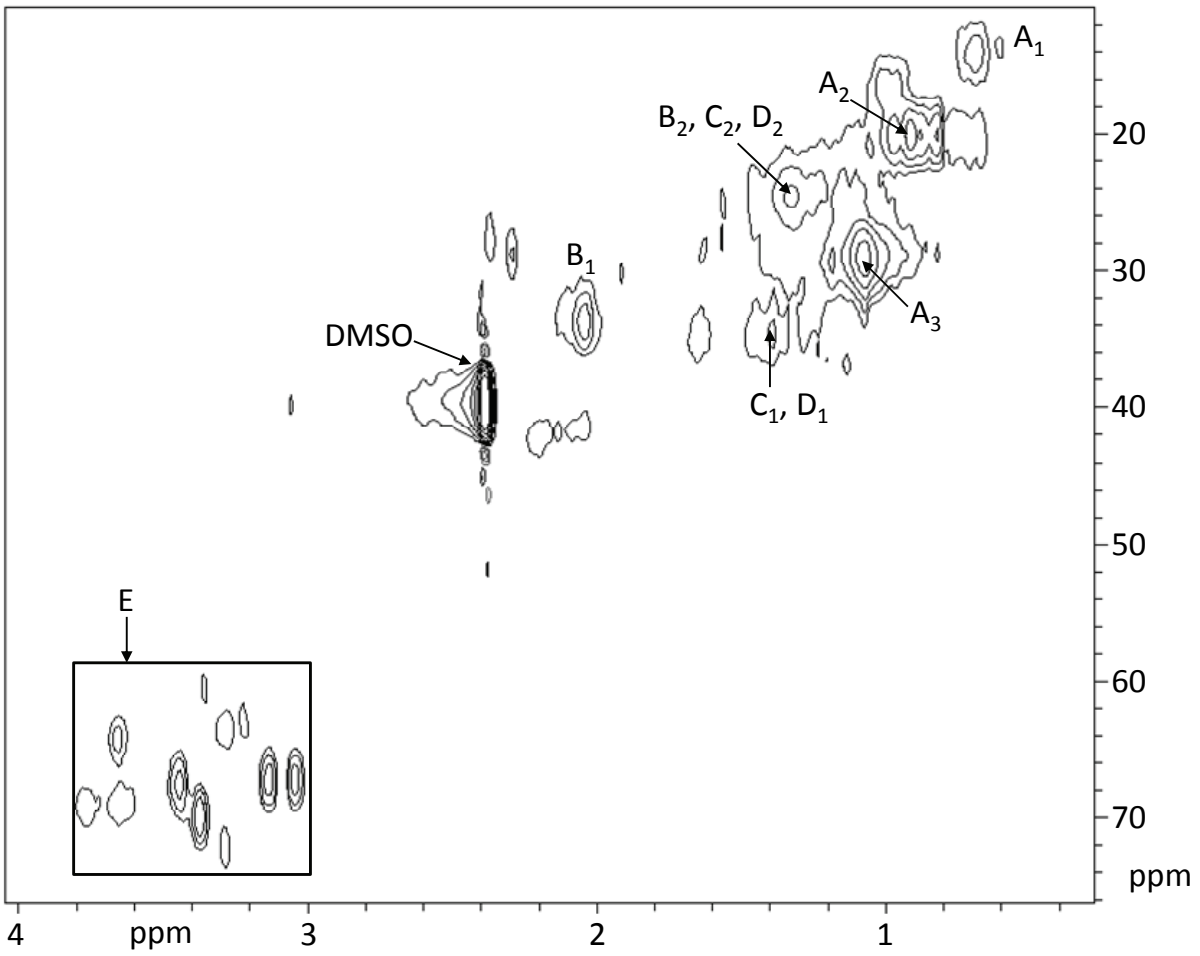

Figure 5: ^{1}H-^{13}C HSQC NMR Spectrum of the Base-Soluble Material from Clay Sample CCP Highlighting Major ^{1}H-^{13}C Couplings Between Aliphatic and *O*-Alkyl Structures. Assignments are explained in Table 8.

3.4 DISCUSSION OF MOLECULAR ANALYSIS

The solvent-extractable NOM was mainly composed of *n*-alkanoic acids, *n*-alkanols and *n*-alkanes of various chain lengths. Potential sources for these compounds can be determined based on biomarker structure. A homologous series of long-chain *n*-alkanoic acids, *n*-alkanols and *n*-alkanes ($\geq C_{20}$) are believed to be biomarkers for vascular plant waxes (Bianchi, 1995). The short chain aliphatic lipids ($<C_{20}$) are generally thought to be derived from different sources based on the type of compound. Short chain *n*-alkanols are derived primarily from microbes (Ficken et al., 2000; Harwood and Russel, 1984) while short-chain *n*-alkanes are biomarkers for both plants and microbes (Harwood and Russel, 1984; Volkman et al., 1998). Short chain *n*-alkanoic acids are derived from microbes, plants or mosses (Baas et al., 2000; Harwood and Russel, 1984; Volkman et al., 1998). Due to the low concentrations of short chain *n*-alkanols observed, the short chain *n*-alkanoic acids detected are more likely derived from plant sources rather than microbial sources. The biomarker ergosterol is also commonly found in NOM solvent

extracts but was not observed in these samples. Ergosterol is most commonly associated with fungi (Feng et al., 2008; Ruzicka et al., 2000) suggesting that the microbial inputs observed in the clay samples are more likely from bacteria rather than fungi.

A variety of ratios that provide additional information about NOM sources can be applied to long-chain *n*-alkanes (Bush and McInerney, 2013; Lei et al., 2010; Nott et al., 2000). Based on the ratio of $C_{29}/(C_{27}+C_{29}+C_{31})$ chain lengths, values of 0.2-0.35 are indicative of grasses and broad leaf tissues while values of 0.35-0.5 indicate conifer-derived tissues (Lei et al., 2010). This proxy was only applied to the MX-80 results because the C_{29} chain length was not observed in the CCP or National samples. The value of 0.40 calculated for MX-80 suggests a dominance of conifer-derived materials. Other proxies are also available which do not include C_{29}. The ratio of $C_{23}/(C_{23}+C_{27})$ is used to differentiate between mosses and higher vascular plants with the C_{23} chain length representing moss inputs (Bush and McInerney, 2013; Nott et al., 2000). A preference towards vascular plants was observed for all three samples. Inputs from grasses and trees can be distinguished using the ratio of $C_{31}/(C_{27}+C_{31})$ with C_{31} representing grass tissues (Bai et al., 2009; Meyers and Ishiwatari, 1993). The *n*-alkanes extracted from the MX-80 and CCP samples show a preference towards tree tissues while the opposite is true of the National sample. These *n*-alkane proxies are very useful for providing additional information about the source of NOM in clays and other environmental samples. However, it was recently suggested that these proxies may vary with location due to variations in the abundance of *n*-alkane chain lengths in a plant group in different regions (Bush and McInerney, 2013). The results of the proxies should therefore be thought of as a guide for potential sources of the solvent-extractable material from these clays.

Possible sources can also be determined for compounds extracted by base hydrolysis. In this case, long-chain *n*-alkanoic acids are thought to be derived from waxes and suberin from vascular plants (Otto and Simpson, 2006b). *α*-Hydoxyalkanoic acids were also found in all three clay samples and are generally thought to be biomarkers for leaf waxes and wood (De Leeuw et al., 1995; Freire et al., 2002). Only the National sample was found to contain *ω*-hydroxyalkanoic acids which are derived from suberin in roots and bark (Kolattukudy and Espelie, 1989) and polyesters in leaf waxes of grasses and conifers (Bull et al., 2000). *α,ω*-Alkanedioic acids were found in the CCP sample and are biomarkers for suberin which is often thought to be an indicator for vascular plants (Kolattukudy and Espelie, 1989). These potential NOM sources are in agreement with the results of the solvent extraction because they point mainly towards microbial and vascular plant sources. The biomarkers indicating leaf waxes, wood and bark are also consistent with inputs from trees.

Of the vanillyl, syringyl and cinnamyl groups that are normally found after CuO chemolysis, only vanillic acid and vanillin were observed in the extracts. Vanillyl-type phenols have been reported to be more environmentally persistent than cinnamyl or syringyl phenols (Hedges et al., 1988), which may explain why only these lignin-derived phenols were observed. The presence of only vanillyl groups may also indicate that this material is derived from a gymnosperm source rather than an angiosperm source which would produce both vanillyl and syringyl groups. The absence of cinnamyl groups may be indicative of woody gymnosperm tissues as opposed to non-woody tissues such as conifer needles (Hedges and Mann, 1979). All of the clay samples contained *α,ω*-alkanedioic acids which are biomarkers for suberin (Kolattukudy and Espelie, 1989). The MX-80 and CCP samples contained *m*- and *p*-hydroxybenzoic acids which are thought to be indicative of plant-derived proteins (Goñi et al., 2000). The extract from sample CCP also contained 3,5-dihydroxybenzoic acid, a biomarker for polyhydroxyaromatic tannins (Prahl et al., 1994). The results of this extraction suggest mainly higher plant sources with the possibility that trees, and more specifically gymnosperms, are large contributors.

The acid to aldehyde ratio (Ad/Al) of vanillyl and syringyl monomers is a commonly used metric to determine the degradation state of lignin in environmental samples (Hedges et al., 1988). Biodegradation of lignin results in oxidation of these monomers (Ten Have and Teunissen, 2001) and thus a higher Ad/Al ratio indicates lignin at a higher state of degradation. Vanillic acid was detected in all three clays but only the extract from the National sample contained vanillin as well at an Ad/Al ratio of 6.88. In fresh woody tissue from conifers, the Ad/Al ratio for vanillyl monomers has been reported in the range of 0.1-0.5 (Cotrim Da Cunha et al., 2001; Hedges and Mann, 1979), suggesting that lignin in the National sample is in a state of advanced degradation.

Basic structural information about the whole sample can be obtained using solid-state ^{13}C NMR (Kögel-Knabner, 2000; Simpson et al., 2008). The spectra obtained for NOM in the MX-80, CCP and National samples have very similar signal intensities in all of the spectral regions. More than 85% of the signal was found in the aliphatic and aromatic regions in all cases. Signal in the aliphatic region corresponds to methylene carbons in proteins, lipids or waxes and the small shoulder at 15 ppm indicates terminal CH_3 groups (Preston et al., 1997; Simpson et al., 2008). The aromatic region represents carbons in lignin, proteins or black carbon (Baldock et al., 1992; Simpson et al., 2008). Based on the results of the CuO oxidation, it is not likely that this signal corresponds to the presence of lignin in the sample as only two of the eight lignin-derived phenols were observed. The 6-7% of the total signal found in the *O*-alkyl region corresponds to methoxy groups in carbohydrates or lignin and the 1-6% of the total signal in the carboxy and carbonyl region may indicate carboxylic, amide or ester groups (Simpson et al., 2008). The ratio of signal intensities in the alkyl and *O*-alkyl regions is another method used to approximate the degree to which NOM has been diagenetically altered (Baldock et al., 1992; Simpson et al., 2008). The alkyl/*O*-alkyl ratios for the MX-80, CCP and National samples were 8.0, 7.6 and 9.7. Even soils with higher levels of NOM degradation generally have an alkyl/*O*-alkyl ratio between 0-2 (Pisani et al., 2013; Simpson et al., 2008). NOM in the clay samples studied has therefore likely undergone a great deal of diagenetic alteration during or post-deposition.

More detailed structural information on NOM samples is often acquired with solution-state ^{1}H NMR which results in higher resolution spectra than solid-state NMR (Simpson et al., 2008). The small organic molecules detected in the base-soluble extract may be by-products of microbial metabolism (Gest, 1981; Schink and Zeikus, 1980). However, it is unclear whether these may be artifacts of past metabolism as no experiments to determine microbial activity were performed. The results of the 1D and 2D solution-state NMR experiments showed that many of the peaks likely correspond to the types of compounds outlined in Table 7. These are mostly long-chain aliphatic compounds with some oxygen functionality. The relative ratio of intensities of the CH_2 (A_2) and CH_3 (A_1) peaks in the 1D spectra indicates that there are not many terminal CH_3 groups which suggests that these compounds also have relatively few side chains. Long-chain aliphatic compounds have been hypothesized to be more recalcitrant due to protection by sorption to the clay surface (Baldock and Skjemstad, 2000; Feng et al., 2005). The large signal observed in the solid-state ^{13}C NMR spectra may indicate that more of these long-chain aliphatics are present but are sorbed too strongly to the clay surface to be removed by the extraction techniques used. Based on the fact that no amino acids were observed in any of the solution-state ^{1}H NMR spectra, it is unlikely that the aromatic signal in the solid-state ^{13}C NMR spectra corresponds to carbon in proteins. This suggests that black carbon or some other non-extractable aromatic-rich NOM is the most likely source of the signal in the aromatic region. Formation of bentonite clays is known to have occurred in the presence of volcanic ash (Fisher and Schmincke, 1984; Grim and Güven, 1978) which has been shown to be largely composed of black carbon-like material (Kramer et al., 2004).

4. CONCLUSIONS

Geochemical analyses were performed to collect data that could be useful in future assessments of potential organic and nutrient sources in a DGR. Overall the geochemical analysis of the five clay samples showed that the MX-80, Asha and RWC samples have the highest CEC values and lowest OC contents. Data on other inorganic nutrients, such as P, S, N and Fe were also collected (Table 1). Comparison to previous analyses of several of these clay samples (Table 2) suggests that there is significant variation in geochemical composition among samples that may occur naturally within the deposits.

Three candidate clay samples were chosen for detailed molecular-level analysis. The two clays from the Wyoming, USA deposit, MX-80 and National, were analyzed as well as CCP from Saskatchewan, Canada. MX-80 is also the current reference clay for the NWMO repository design (Villagran et al., 2011). Characterization of NOM at the molecular-level in clay samples MX-80, National and CCP from Wyoming and Saskatchewan identified very similar sources between samples. Major inputs from microbes and vascular plants were detected with microbial inputs likely from bacteria due to a lack of observed fungal biomarkers. Vascular plant inputs likely represent a much larger fraction of the solvent-extractable compounds than microbial inputs. The solid-state ^{13}C NMR spectra were dominated by signal in the aliphatic and aromatic regions. The results of the 1D and 2D solution-state NMR allowed for further characterization of this material as long-chain aliphatic compounds with minimal branching and aromatic carbon that is likely in the form of black carbon. Based on degradation ratios, the NOM present in these clays has undergone substantial diagenetic alteration. The remaining NOM is composed mainly of compounds that are hypothesized to be recalcitrant due to their inherent chemical structure as well as physical protection by the clay surface due to sorptive interactions.

The composition of NOM found in the three clays analyzed was very similar based on the biomarker, solid-state and solution-state NMR experiments. NOM was observed to be in a highly degraded state and was mainly composed of long-chain aliphatic carbon with minimal side branching and aromatic carbon. These compounds are hypothesized to be recalcitrant and likely have strong interactions with the surface of the clay minerals. Based on this molecular-level analysis, the NOM is predominantly recalcitrant and is not a labile C source for microbes. However, to further confirm if this type of NOM can act as a microbial substrate, future experiments should test this using conventional incubation experiments and re-analysis of NOM to determine if biodegradation has occurred.

ACKNOWLEDGEMENTS

The Asha and Ibeco RWC clay samples were generously provided by Patrik Sellin of the Swedish Nuclear Fuel and Waste Management Company (SKB). The authors also thank Prof. André Simpson and Dr. R. Soong for assistance with NMR data acquisition.

REFERENCES

Anderson, K.A. 1996. A micro-digestion and analysis method for the determination of macro and micro elements in plant tissue by inductively coupled plasma atomic emission spectrometry. Atomic Spectroscopy 1: 30.

Baas, M., R. Pancost, B. Van Geel and J.S. Sinninghe Damsté. 2000. A comparative study of lipids in sphagnum species. Organic Geochemistry 31: 535-541.

Bai, Y., X. Fang, J. Nie, Y. Wang and F. Wu. 2009. A preliminary reconstruction of the paleoecological and paleoclimatic history of the Chinese loess plateau from the application of biomarkers. Palaeogeography, Palaeoclimatology, Palaeoecology 271: 161-169.

Baldock, J.A., J.M. Oades, A.G. Waters, X. Peng, A.M. Vassallo and M.A. Wilson. 1992. Aspects of the chemical structure of soil organic materials as revealed by solid-state ^{13}C NMR spectroscopy. Biogeochemistry 16: 1-42.

Baldock, J.A. and J.O. Skjemstad. 2000. Role of the soil matrix and minerals in protecting natural organic materials against biological attack. Organic Geochemistry 31: 697-710.

Bianchi, G. 1995. Plant waxes. *In*: Waxes: Chemistry, Molecular Biology and Functions (R.J. Hamilton, Ed.). The Oily Press, Dundee, pp: 175-222.

Bors, J.,S. Dultz and B. Riebe. 1999. Retention of radionuclides by organophilic bentonite. Engineering Geology 54: 195-206.

Bull, I.D., C.J. Nott, P.F. Van Bergen, P.R. Poulton and R.P. Evershed. 2000. Organic geochemical studies of soils from the Rothamsted classical experiments - VI. The occurrence and source of organic acids in an experimental grassland soil. Soil Biology and Biochemistry 32: 1367-1376.

Bush, R.T. and F.A. McInerney. 2013. Leaf wax n-alkane distributions in and across modern plants: Implications for paleoecology and chemotaxonomy. Geochimica Et Cosmochimica Acta 117: 161-179.

Clemente, J.S., E.G. Gregorich, A.J. Simpson, R. Kumar, D. Courtier-Murias and M.J. Simpson. 2012. Comparison of nuclear magnetic resonance methods for the analysis of organic matter composition from soil density and particle fractions. Environmental Chemistry 9: 97-107.

Conte, P., R. Spaccini and A. Piccolo. 2004. State of the art of CPMAS ^{13}C-NMR spectroscopy applied to natural organic matter. Progress in Nuclear Magnetic Resonance Spectroscopy 44: 215-223.

Cotrim Da Cunha, L., L. Serve, F. Gadel and J. Blazi. 2001. Lignin-derived phenolic compounds in the particulate organic matter of a French Mediterranean river: Seasonal and spatial variations. Organic Geochemistry 32: 305-320.

Dass, C. 2007. Fundamentals of contemporary mass spectrometry. Wiley-Interscience, Hoboken, N.J.

De Leeuw, J W., W. Irene, C. Rijpstra and P.H. Nienhuis. 1995. Free and bound fatty acids and hydroxy fatty acids in the living and decomposing eelgrass zostera marina L. Organic Geochemistry 23: 721-728.

Deshmukh, A.P., A.J. Simpson and P.G. Hatcher. 2003. Evidence for cross-linking in tomato cutin using HR-MAS NMR spectroscopy. Phytochemistry 64: 1163-1170.

Feng, X., A.J. Simpson and M.J. Simpson. 2005. Chemical and mineralogical controls on humic acid sorption to clay mineral surfaces. Organic Geochemistry 36: 1553-1566.

Feng, X., A.J. Simpson, K.P. Wilson, D. Dudley Williams and M.J. Simpson. 2008. Increased cuticular carbon sequestration and lignin oxidation in response to soil warming. Nature Geoscience 1: 836-839.

Feng, X. and M.J. Simpson. 2011. Molecular-level methods for monitoring soil organic matter responses to global climate change. Journal of Environmental Monitoring 13: 1246-1254.

Ficken, K.J., B. Li, D.L. Swain and G. Eglinton. 2000. An n-alkane proxy for the sedimentary input of submerged/floating freshwater aquatic macrophytes. Organic Geochemistry 31: 745-749.

Fisher, R.V. and H.U. Schmincke, 1984. Pyroclastic rocks. Springer-Verlag, Berlin.

Freire, C.S.R., A.J.D. Silvestre and C. Pascoal Neto. 2002. Identification of new hydroxy fatty acids and ferulic acid esters in the wood of eucalyptus globulus. Holzforschung 56: 143-149.

Gest, H. 1981. Evolution of the citric acid cycle and respiratory energy conversion in prokaryotes. FEMS Microbiology Letters 12: 209-215.

Gonclaves, C.N., R.D.S. Dalmolin, D.P. Dick, H. Knicker, E. Klamt and I. Kögel-Knabner. 2003. The effect of 10% HF treatment on the resolution of CPMAS ^{13}C NMR spectra and on the quality of organic matter in ferralsols. Geoderma 116: 373-392.

Goñi, M.A., M.B. Yunker, R.W. MacDonald and T.I. Eglinton. 2000. Distribution and sources of organic biomarkers in arctic sediments from the Mackenzie river and Beaufort shelf. Marine Chemistry 71: 23-51.

Grim, R.E. and N. Güven, 1978. Bentonites: Geology, mineralogy, properties and uses. Elsevier Scientific Publishing Company, Amsterdam; New York.

Hallbeck, L. 2010. Principal organic materials in a repository for spent nuclear fuel. Swedish Nuclear Fuel and Waste Management Company Technical Report TR-10-19. Stockholm, Sweden.

Harwood, J.L. and N.J. Russell. 1984. Lipids in plants and microbes. George Allen and Unwin, London.

Hedges, J.I., R.A. Blanchette, K. Weliky and A.H. Devol. 1988. Effects of fungal degradation on the CuO oxidation products of lignin: A controlled laboratory study. Geochimica Et Cosmochimica Acta 52: 2717-2726.

Hedges, J.I. and D.C. Mann. 1979. The characterization of plant tissues by their lignin oxidation products. Geochimica Et Cosmochimica Acta 43: 1803-1807.

Hicks, T W., M.J. White and P.J. Hooker. 2009. Role of bentonite in determination of thermal limits on geological disposal facility design. Galson Sciences Limited Technical Report 0883-1. Oakham, Tutland.

Jung, S., D.A. Rickert, N.A. Deak, E.D. Aldin, J. Recknor, L.A. Johnson and P.A. Murphy. 2003. Comparison of Kjeldahl and Dumas Methods for Determining Protein Contents of Soybean Products. JAOCS 80: 1169-1173.

Karnland, O. 2010. Chemical and mineralogical characterization of the bentonite buffer for the acceptance control procedure in a KBS-3 repository. Swedish Nuclear Fuel and Waste Management Company Technical Report TR-10-60. Stockholm, Sweden.

Keto, P. 2003. Natural clays as backfilling materials in different backfilling concepts. Posiva Oy Working Report 2003-79. Eurajoki, Finland.

Kiviranata, L. and S. Kumpulainen. 2011. Quality control and characterization of bentonite materials. Posiva Oy Working Report 2011-84. Eurajoki, Finland.

Kögel-Knabner, I. 2000. Analytical approaches for characterizing soil organic matter. Organic Geochemistry 31: 609-625.

Kolattukudy, P. and K. Espelie. 1989. Chemistry, biochemistry, and function of suberin and associated waxes. *In*: Natural Products of Woody Plants (J. Rowe, Ed.). Springer Berlin Heidelberg, pp: 304-367.

Kozai, N. 1998. Sorption characteristics of americium on buffer material. *In*: Progress Report on Safety Research on Radioactive Waste Management for the Period April 1996 to March 1998 (T. Ohnuki, S. Muraoka and T. Banba, Eds.). Japan Atomic Energy Research Institute Review 98-014. Ibaraki, Japan, pp: 21.

Kramer, R.W., E.B. Kujawinski and P.G. Hatcher. 2004. Identification of black carbon derived structures in a volcanic ash soil humic acid by fourier transform ion cyclotron resonance mass spectrometry. Environmental Science and Technology 38: 3387-3395.

Kumpulainen, S. and L. Kiviranta. 2010. Mineralogical and chemical characterization of various bentonite and smectite-rich clay materials. Posiva Oy Working Report 2010-52. Eurajoki, Finland.

Lei, G., H. Zhang, F. Chang, Y. Pu, Y. Zhu, M. Yang and W. Zhang. 2010. Biomarkers of modern plants and soils from Xinglong mountain in the transitional area between the Tibetan and loess plateaus. Quaternary International 218: 143-150.

Liang, J. and R.E. Karamanos. 1993. DPTA-Extractable Fe, Mn, Cu and Zn. *In*: Soil Sampling and Methods of Analysis (M.R. Carter, Ed.). Canadian Society of Soil Science. Lewis Publishers.

Mariner, P., J. Lee, E. Hardin, F. Hansen, G. Freeze, A. Lord, B. Goldstein and R. Price. 2011. Granite disposal of U.S. high-lever radioactive waste. Sandia National Laboratories Scientific Report SAND2011-6203. Albuquerque, New Mexico.

Marshall, M.H.M. and M.J. Simpson. 2014. State of Science Review: Organic Matter in Clays and Groundwater. Nuclear Waste Management Organization, Technical Report NWMO TR-2014-05. Toronto, Ontario.

Meyers, P.A. and R. Ishiwatari. 1993. Lacustrine organic geochemistry-an overview of indicators of organic matter sources and diagenesis in lake sediments. Organic Geochemistry 20: 867-900.

MOE. 2007. The Determination of Trace Metals in Soil, Compost, Liquid Effluent and Solid Industrial Waste By the Spectro Inductively Coupled Plasma-Optical Emission Spectrometer (ICP-OES). Ministry of Environment Laboratory Services Branch. HMPSOIL-E3073. Toronto, Ontario.

Moulin, V. and G. Ouzounian. 1992. Role of colloids and humic substances in the transport of radio elements through the geosphere. Applied Geochemistry 179-186.

Nelson, D. W. and L.E. Sommers. 1982. Total carbon, organic carbon, and organic matter, 29-2.2.4 method using high-temperature induction furnace. 549-552.

Nirex. 2006. Potential areas of future geosphere research. United Kingdom Nirex Limited Technical Note 494794. Didcot, Oxfordshire.

Nott, C.J., S. Xie, L.A. Avsejs, D. Maddy, F.M. Chambers and R.P. Evershed. 2000. n-alkane distributions in ombrotrophic mires as indicators of vegetation change related to climatic variation. Organic Geochemistry 31: 231-235.

O'Dell, J.W. 1993. Determination of Nitrate-Nitrite Nitrogen by Automated Colorimetry. United States Environmental Protection Agency 600/R93/100: Method 353.2.

Olsson, S. and O. Karnland. 2009. Characterisation of bentonites from Kutch, India and Milos, Greece - some candidate tunnel back-fill materials? Swedish Nuclear Fuel and Waste Management Company R-09-53. Stockholm, Sweden.

Oscarson, D.W., S. Stroes-Gascoyne and S.C.H. Cheung. 1986. The effect of organic matter in clay sealing materials on the performance of a nuclear fuel waste disposal vault. Atomic Energy of Canada Limited Technical Report AECL-9078. Pinawa, Manitoba.

Otto, A. and M.J. Simpson. 2005. Degradation and preservation of vascular plant-derived biomarkers in grassland and forest soils from western Canada. Biogeochemistry 74: 377-409.

Otto, A. and M.J. Simpson. 2006a. Evaluation of CuO oxidation parameters for determining the source and stage of lignin degradation in soil. Biogeochemistry 80: 121-142.

Otto, A. and M.J. Simpson. 2006b. Sources and composition of hydrolysable aliphatic lipids and phenols in soils from western Canada. Organic Geochemistry 37: 385-407.

Pearce, R. and P. Drouin. 2008. The Determination of Arsenic, Selenium and Antimony in Trade Wastes, Compost, Soils, Sediments and Vegetation by Hydride-Flameless Atomic Absorption Spectrophotometry (HYD-FAAS). Ministry of Environment Laboratory Services Branch. HYDPSSV-E3245.

Pisani, O., K.M. Hills, D. Courtier-Murias, A.J. Simpson, N.J. Mellor, E.A. Paul, S.J. Morris and M.J. Simpson. 2013. Molecular level analysis of long term vegetative shifts and relationships to soil organic matter composition. Organic Geochemistry 62: 7-16.

Prahl, F.G., J.R. Ertel, M.A. Goñi, M.A. Sparrow and B. Eversmeyer. 1994. Terrestrial organic carbon contributions to sediments on the Washington margin. Geochimica Et Cosmochimica Acta 58: 3035-3048.

Preston, C.M., J.A. Trofymow, B.G. Sayer and J. Niu. 1997. ^{13}C nuclear magnetic resonance spectroscopy with cross-polarization and magic-angle spinning investigation of the proximate-analysis fractions used to assess litter quality in decomposition studies. Canadian Journal of Botany 75: 1601-1613. Reid, K. 1998. Soil Fertility Handbook. OMAFRA Publication.

Reid, K. (Ed.) 1998. Soil Fertility Handbook. OMAFRA Publication.

Rhoades, J.D. 1982. Cation Exchange Capacity. *In*: Methods of Soil Analysis Part 2, Second Edition, Agronomy 9, Part 2 (A.L. Page, Ed.). American Society of Agronomy, Inc. Madison.

Rumpel, C., N. Rabia, S. Derenne, K. Quenea, K. Eusterhues, I. Kögel-Knabner and A. Mariotti. 2006. Alteration of soil organic matter following treatment with hydrofluoric acid (HF). Organic geochemistry 37: 1437-1451.

Russell, D. and R. Pearce. 2009. The Determination of Mercury in Soils, Sediments and Vegetation by Cold Vapour-Atomic Absorption Spectrophotometry (CV-AAS). Ministry of Environment Laboratory Services Branch. HGSSV-E3059.

Ruzicka, S., D. Edgerton, M. Norman and T. Hill. 2000. The utility of ergosterol as a bioindicator of fungi in temperate soils. Soil Biology and Biochemistry 32: 989-1005.

Schink, B. and J.G. Zeikus. 1980. Microbial methanol formation - a major end product of pectin metabolism. Current Microbiology 4: 387-389.

Schmidt, M.W.I, H. Knicker, P.G. Hatcher and I. Kögel-Knabner. 1997. Improvement of ^{13}C and ^{15}N CPMAS NMR spectra of bulk soils, particle size fractions and organic material by treatment with hydrofluoric acid (10%). European Journal of Soil Science 48: 319-328.

Schmidt, M.W.I., M. S. Torn, S. Abiven, T. Dittmar, G. Guggenberger, I. A. Janssens, M. Kleber, I. Kögel-Knabner, J. Lehmann, D. A. C. Manning, P. Nannipieri, D. P. Rasse, S. Weiner and S. E. Trumbore. 2011. Persistence of soil organic matter as an ecosystem property. Nature 478: 49-56.

Simard, R.R. 1993. Ammonium Acetate-Extractable Elements. *In*: Soil Sampling Methods of Analysis (M.R. Carter, Ed.). Canadian Society of Soil Science. Lewis Publishers.

Simoneit, B.R.T., V.O. Elias, M. Kobayashi, K. Kawamura, A.I. Rushdi, P.M. Medeiros, W.F. Rogge and B.M. Didyk. 2004. Sugars - Dominant water-soluble organic compounds in soils and characterization as tracers in atmospheric particulate matter. Environmental Science and Technology 38: 5939-5949.

Simoneit, B.R.T. 2005. A review of current applications of mass spectrometry for biomarker/molecular tracer elucidations. Mass Spectrometry Reviews 24: 719-765.

Simpson, A.J. and S.A. Brown. 2005. Purge NMR: Effective and easy solvent suppression. Journal of Magnetic Resonance 175: 340-346.

Simpson, A.J., W.L. Kingery and P.G. Hatcher. 2003. The identification of plant derived structures in humic materials using three-dimensional NMR spectroscopy. Environmental Science and Technology 37: 337-342.

Simpson, M.J., A. Otto and X. Feng. 2008. Comparison of solid-state carbon-13 nuclear magnetic resonance and organic matter biomarkers for assessing soil organic matter degradation. Soil Science Society of America Journal 72: 268-276.

SKB. 2006. Long-term safety for KBS-3 repositories at forsmark and laxemar - a first evaluation. Main report of the SR-can project. Swedish Nuclear Fuel and Waste Management Company Technical Report TR-06-09. Stockholm, Sweden.

Stroes-Gascoyne, S., C.J. Hamon and P. Maak. 2011. Limits to the use of highly compacted bentonite as a deterrent for microbiologically influenced corrosion in a nuclear fuel waste repository. Physics and Chemistry of the Earth 36: 1630-1638.

Stroes-Gascoyne, S., C.J. Hamon, P. Maak and S. Russell. 2010. The effects of the physical properties of highly compacted smectitic clay (bentonite) on the culturability of indigenous microorganisms. Applied Clay Science 47: 155-162.

Stroes-Gascoyne, S. and J. West. 1997. Microbial studies in the Canadian nuclear fuel waste management program. FEMS Microbiology Reviews 20: 573-590.

Svensson, D., A. Dueck, S. Lydmark and S. Hansen. 2011. Alternative buffer material – status of the ongoing laboratory investigation of reference materials and test package 1.Swedish Nuclear Fuel and Waste Management Company Technical Report TR-11-06. Stockholm, Sweden.

Ten Have, R. and P.J.M. Teunissen. 2001. Oxidative mechanisms involved in lignin degradation by white-rot fungi. Chemical Reviews 101: 3397-3413.

Villagran, J., M. Ben Belfadhel, K. Birch, J. Freire-Canosa, M. Garamszeghy, F. Garisto, P. Gierszewski, M. Gobien, S. Hirschorn, N. Hunt, A. Khan, E. Kremer, G. Kwong, T. Lam, P. Maak, J. McKelvie, C. Medri, A. Murchison, S. Russell, M. Sanchez-Rico Castejon, U. Stahmer, E. Sykes, A. Urrutia-Bustos, A. Vorauer, T. Wanne and T. Yang. 2011. RD&D program 2011 - NWMO'S program for research, development and demonstration for long-term management of used nuclear fuel. Nuclear Waste Management Organization, Technical Report NWMO TR-2011-01. Toronto, Ontario.

Volkman, J.K., S.M. Barrett, S I. Blackburn, M P. Mansour, E.L. Sikes and F. Gelin. 1998. Microalgal biomarkers: A review of recent research developments. Organic Geochemistry 29: 1163-1179.

Wilson, J., D. Savage, A. Bond, S. Watson, R. Pusch and D. Bennett. 2011. Bentonite: A review of key properties, processes and issues for consideration in the UK context. Quintessa Technical Report QRS-1378ZG-1. Oxfordshire, UK.

Woods, G.C., M.J. Simpson, P.J. Koerner, A. Napoli and A.J. Simpson. 2011. HILIC-NMR: Toward the identification of individual molecular components in dissolved organic matter. Environmental Science and Technology 45: 3880-3886.